

Enhancing stationary entanglement between two optomechanical oscillators by Coulomb interaction with Kerr medium

Tian-Le Yang(杨天乐), Chen-Long Zhu(朱陈龙), Sheng Liu(刘声), and Ye-Jun Xu(许业军)
Citation: Chin. Phys. B, 2021, 30 (**12**): 124201. DOI: 10.1088/1674-1056/abff3e
Journal homepage: http://cpb.iphy.ac.cn; http://iopscience.iop.org/cpb

What follows is a list of articles you may be interested in

Enhancing stationary entanglement between two optomechanical oscillators by Coulomb interaction with Kerr medium

Tian-Le Yang(杨天乐), Chen-Long Zhu(朱陈龙), Sheng Liu(刘声), and Ye-Jun Xu(许业军)
Chin. Phys. B, 2021, 30 (**12**): 124201. DOI: 10.1088/1674-1056/abff3e

Dissipative dynamics of an entangled three-qubit system via non-Hermitian Hamiltonian: Its correspondence with Markovian and non-Markovian regimes

M Rastegarzadeh and M K Tavassoly
Chin. Phys. B, 2021, 30 (**3**): 034205. DOI: 10.1088/1674-1056/abc2c3

Nonclassicality of photon-modulated atomic coherent states in the Schwinger bosonic realization

Jisuo Wang(王继锁), Xiangguo Meng(孟祥国), and Xiaoyan Zhang(张晓燕)
Chin. Phys. B, 2020, 29 (**12**): 124213. DOI: 10.1088/1674-1056/abb3e8

Quantum speed limit time and entanglement in a non-Markovian evolution of spin qubits of coupled quantum dots

M. Bagheri Harouni
Chin. Phys. B, 2020, 29 (**12**): 124203. DOI: 10.1088/1674-1056/abab75

Reversion of weak-measured quantum entanglement state

Shao-Jiang Du(杜少将), Yonggang Peng(彭勇刚), Hai-Ran Feng(冯海冉), Feng Han(韩峰), Lian-Wu Yang(杨连武), Yu-Jun Zheng(郑雨军)
Chin. Phys. B, 2020, 29 (**7**): 074202. DOI: 10.1088/1674-1056/ab8c3e

---

Enhancing stationary entanglement between two optomechanical oscillators by Coulomb interaction with Kerr medium*

Tian-Le Yang(杨天乐), Chen-Long Zhu(朱陈龙), Sheng Liu(刘声), and Ye-Jun Xu(许业军)†

International Research Center of Quantum Information and Photoelectric Information, School of Mechanical and Electronic Engineering, Chizhou University, Chizhou 247000, China

(Received 14 March 2021; revised manuscript received 24 April 2021; accepted manuscript online 10 May 2021)

We theoretically study the stationary entanglement of two charged nanomechanical oscillators coupling via Coulomb interaction in an optomechanical system with an additional Kerr medium. We show that the degree of entanglement between two nanomechanical oscillators is suppressed by Kerr interaction due to photon blockade and enhanced by Coulomb coupling strength. We also show other parameters for adjusting and obtaining entanglement, such as the driving power and the frequencies of the two oscillators, and the entanglement is robust against temperature. Our study proves a way for adjusting stationary entanglement between two optomechanical oscillators by Coulomb interaction and Kerr medium.

Keywords: entanglement, Kerr interaction, Coulomb interaction, optomechanics

PACS: 42.50.Pq, 03.65.Ud, 42.50.Dv **DOI:** 10.1088/1674-1056/abff3e

1. Introduction

Quantum entanglement is one of inherently physical phenomena that it is considered to be important resource not only in quantum information processing,[1–6] e.g., performing communication and computation tasks with an efficiency which is unachievable in classical world,[7,8] but also in setting the transition between classical and quantum world.[9–11] As a basic feature of quantum theory, quantum entanglement is a significant resource of quantum network that allows the inseparable quantum correlation to be shared between distant parties.[12,13] The generation of quantum entanglement is a crucial task in quantum information processing. Many methods for generating quantum entanglement have been proposed,[14–21] in which the principle of Schrödinger's cat is often the basis of experimental proposals to observe macrosopic quantum entanglement.[22] More recently entanglement has been experimentally achieved in microscopic objects such as photons, phonons and atoms.[23,24]

A cavity optomechanical system is an ideal platform for preparation of entangled states. Over the past few years, due to its unique applications, the research on entangled states has attracted considerable interest, such as the high-sensitivity detection of small masses or forces with the precision of quantum limits.[25–30] A standard optomechanical system is composed of a movable mirror coupling to a Fabry–Pérot cavity by the radiation pressure force. The variant based on the standard optomechanics is abundant, for example, nanoelectromechanical systems formed by a microwave cavity capacitively coupling to a nanoresonator,[31] cavity optomechanics with stoichiometric SiN films,[32] and a semitransparent membrane within a standard Fabry–Pérot cavity.[33,34] More recently, many hybrid optomechanical systems have emerged, including a hybrid cavity magnomechanical system,[23] an atomic ensemble placed within an optical Fabry–Pérot cavity,[35,36] a nonlinear Kerr medium inside an optomechanical cavity, and so on.[33] Especially, the effect of Kerr medium on the dynamics of optomechanical systems was extensively investigated.[37–40] Generally, the entanglement in optomechanical systems is limited by photon blockade mechanism.[41–44]

Here, we consider an optomechanical cavity coupling to an external nanomechanical oscillator (NMO) and the cavity is additionally filled with a Kerr medium.[45–47] The range of interaction distance is from nanometer to meter due to the Coulomb coupling,[48,49] and the strength can be adjusted by the bias voltage.[50,51] We primarily discuss the effect of Kerr interaction and Coulomb coupling strength on the stationary optomechanical entanglement. The entanglement is enhanced with increasing the Coulomb coupling strength. In consideration of Kerr interaction, this leads to the photon blockade, which will lower the entanglement. Utilizing the adjustability of Kerr interaction and Coulomb coupling strength, it is easy to accomplish the transformation between different degrees of entanglement. All entanglements are robust against environmental temperature. We use the standard Langevin formalism to model the system, solve the linearized dynamics and quantify the entanglement in the stationary state. Compared with a related research in Ref. [51], which models a hybrid optomechanical system with a Fabry–Pérot cavity coupling an external NMO through Coulomb force for studying the entanglements between two NMOs, here our work considers that the cavity is additionally filled with a Kerr medium. We mainly demonstrate the influences of Kerr interaction, Coulomb cou-

*Project supported by the National Natural Science Foundation of China (Grant No. 11704051).

†Corresponding author. E-mail: yejunxu@126.com

© 2021 Chinese Physical Society and IOP Publishing Ltd

pling strength and cavity decay rate, i.e., on the entanglement between two NMOs. We also show the effects of Kerr interaction and Coulomb coupling on the entanglement among cavity and NMO_1. Even in the absence of Kerr interaction, weak degree of entanglement can be detected among them.

2. Model and steady state solutions

We consider an optomechanical cavity filling with the Kerr medium coupling to an external nanomechanical oscillator via Coulomb interaction, as shown in Fig. 1. One strong pump field with frequency $\omega_{\rm p}$ is injected into a high quality Fabry–Pérot cavity with frequency $\omega_{\rm c}$. The cavity is composed of a fixed mirror and a movable mirror NMO_1, which is charged by the bias gate voltage V_1 and subject to the Coulomb force due to another charged NMO_2 with the bias gate voltage $-V_2$. Here r_0 is the equilibrium distance between the two NMOs.

The Hamiltonian of the system reads

$$H/\hbar = \Delta_{\rm c}c^{\dagger}c+\frac{\omega_1}{2}(p_1^2+q_1^2)+\frac{\omega_2}{2}(p_2^2+q_2^2) -gc^{\dagger}cq_1+\lambda q_1q_2+{\rm i}\varepsilon_{\rm p}(c^{\dagger}-c)+\frac{1}{2}\chi c^{\dagger 2}c^2, \quad (1)$$

where $\Delta_{\rm c}=\omega_{\rm c}-\omega_{\rm p}$ respresents the detuning of pump field from the bare cavity, c and $c^{\dagger}$ are the annihilation and creation operators of the cavity mode with the commutation relation $\left[c,c^{\dagger}\right]=1$, $q_1(q_2)$ and $p_1(p_2)$ are the dimensionless position and momentum quadratures of the charged NMO_1 (NMO_2) with the commutation relation $[q_1,p_1]={\rm i}$ ($[q_2,p_2]={\rm i}$); ω_1 (ω_2) and m_1 (m_2) are the resonance frequency and effective mass of the charged NMO_1 (NMO_2). The coupling parameter between NMO_1 and the cavity field is $g=\omega_{\rm c}/L\sqrt{\hbar/m\omega_1}$ with L being the cavity length and m the mechanical mass. Here, $\lambda=C_1V_1C_2V_2/(2\pi\hbar\varepsilon_0r_0^3)$ is the Coulomb coupling strength between the charged NMO_1 and NMO_2, where the NMO_1 and NMO_2 take the charges $Q_1=C_1V_1$ and $Q_2=-C_2V_2$, with $C_1(C_2)$ and $V_1(-V_2)$ being the capacitance and the voltage of the bias gate, respectively. The strong pump field possesses the frequency $\omega_{\rm p}$ and the amplitude $\varepsilon_{\rm p}=\sqrt{2\kappa P/\hbar\omega_{\rm p}}$, with P being the power of the pump field and κ the cavity decay rate. Giant optical Kerr nonlinearities are obtained by placing a $\xi^{(3)}$ medium inside a cavity,[52] with the Kerr parameter $\chi=3\omega_{\rm c}^2\,{\rm Re}[\xi^{(3)}]/2\varepsilon_0V_{\rm c}$, ε_0 being the dielectric constant of the medium, $V_{\rm c}$ the volume of the cavity, and $\xi^{(3)}$ the third-order nonlinear susceptibility.

The quantum Langevin equations (QLEs) describing the system are given by

$$\dot{q}_1 = \omega_1p_1, \quad (2)$$

$$\dot{p}_1 = -\omega_1q_1-\gamma_1p_1+gc^{\dagger}c-\lambda q_2+\xi_1, \quad (3)$$

$$\dot{q}_2 = \omega_2p_2, \quad (4)$$

$$\dot{p}_2 = -\omega_2q_2-\gamma_2p_2-\lambda q_1+\xi_2, \quad (5)$$

$$\dot{c} = -(\kappa+{\rm i}\Delta_{\rm c})c+{\rm i}gq_1c-{\rm i}\chi c^{\dagger}c^2+\varepsilon_{\rm p}+\sqrt{2\kappa}c_{\rm in}, \quad (6)$$

where γ_1 (γ_2) is the decay rate for NMO_1 (NMO_2). The quantum Brownian noise ξ_1 (ξ_2) comes from the coupling between NMO_1 (NMO_2) and its own environment, whose correlation function can be approximately written as $\langle\xi(t)\,\xi(t')\rangle\simeq\gamma_{\rm m}(2\bar{n}+1)\,\delta(t-t')$, where a non-Markovian Brownian force approximation has been made when the experimentally realizable quality factor $Q_{\rm m}=\omega_{\rm m}/\gamma_{\rm m}$ is very high, up to 10^6.[53] Here $\bar{n}=[\exp(\hbar\omega_{\rm m}/k_{\rm B}T)-1]^{-1}$ is the mean number of thermal excitation, with $k_{\rm B}$ the Boltzmann constant and T the environmental temperature, and $c_{\rm in}$ is the input vacuum noise operator with nonzero correlation function $\langle c_{\rm in}(t)\,c_{\rm in}^{\dagger}(t')\rangle=\delta(t-t')$.

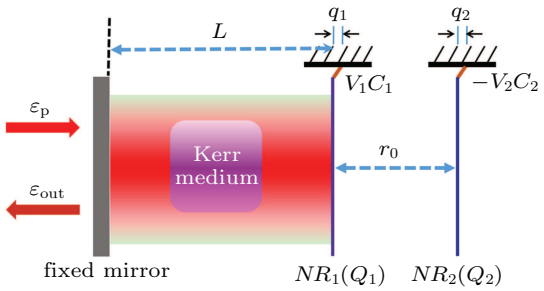


Fig. 1. The sketch of the optomechanical system. The cavity contains the Kerr medium.

Using a standard method in quantum optics, we take the expectation with respect to the steady state of Eqs. (2)–(6).[54–57] Neglecting all the fluctuations, we set

$$\frac{{\rm d}\langle p_1\rangle_{\rm s}}{{\rm d}t}=\frac{{\rm d}\langle q_1\rangle_{\rm s}}{{\rm d}t}=\frac{{\rm d}\langle p_2\rangle_{\rm s}}{{\rm d}t}=\frac{{\rm d}\langle q_2\rangle_{\rm s}}{{\rm d}t}=\frac{{\rm d}\langle c\rangle_{\rm s}}{{\rm d}t}=0,$$

where the subscript s denotes the steady-state value ($\langle p_1\rangle_{\rm s}=p_{1{\rm s}}$, $\langle q_1\rangle_{\rm s}=q_{1{\rm s}}$, $\langle p_2\rangle_{\rm s}=p_{2{\rm s}}$, $\langle q_2\rangle_{\rm s}=q_{2{\rm s}}$ and $\langle c\rangle_{\rm s}=c_{\rm s}$). The steady state solutions are given by $p_{1{\rm s}}=p_{2{\rm s}}=0$, $q_{1{\rm s}}=g|c_{\rm s}|^2/\left(\omega_1+\lambda^2/\omega_2\right)$, $q_{2{\rm s}}=-\lambda q_{1{\rm s}}/\omega_2$, $c_{\rm s}=\varepsilon_{\rm p}/(\kappa+{\rm i}\Delta)$, where $\Delta=\Delta_{\rm c}-gq_{1{\rm s}}+\chi|c_{\rm s}|^2$. Since the pump field is strong, the cavity field has a large amplitude $|c_{\rm s}|\gg1$, which allows us to linearize the dynamics of the system around the steady-state values by writing any operators as $c=c_{\rm s}+\delta c$, $q_i=q_{i{\rm s}}+\delta q_i$ and $p_i=p_{i{\rm s}}+\delta p_i$ ($i=1,2$) and neglecting second order fluctuation terms, such as $\delta c^{\dagger}\delta c$. The QLEs of the fluctuational operators read

$$\delta\dot{q}_1 = \omega_1\delta p_1, \quad (7)$$

$$\delta\dot{p}_1 = -\omega_1\delta q_1-\gamma_1\delta p_1+\sqrt{2}gc_{\rm s}\delta X-\lambda\delta q_2+\xi_1, \quad (8)$$

$$\delta\dot{q}_2 = \omega_2\delta p_2, \quad (9)$$

$$\delta\dot{p}_2 = -\omega_2\delta q_2-\gamma_2\delta p_2-\lambda\delta q_1+\xi_2, \quad (10)$$

$$\delta\dot{c} = -(\kappa+{\rm i}\Delta_{\rm c})\delta c+{\rm i}g(c_{\rm s}\delta q_1+q_{1{\rm s}}\delta c) -{\rm i}\chi(c_{\rm s}^2\delta c^{\dagger}+|c_{\rm s}|^2\,\delta c)+\sqrt{2\kappa}c_{\rm in}. \quad (11)$$

3. Entanglement

In the following, we aim at investigating the NMO-NMO entanglement of the system containing the Kerr medium. The linearized QLEs describing the quadrature fluctuations $(\delta q_1, \delta p_1, \delta q_2, \delta p_2, \delta X, \delta Y)$, with $\delta X = \left(\delta c + \delta c^\dagger\right)/\sqrt{2}$, $\delta Y = \mathrm{i}\left(\delta c^\dagger - \delta c\right)/\sqrt{2}$, can be written as $\dot{u}(t) = Au(t) + n(t)$, where

$$u(t) = [\delta q_1(t), \delta p_1(t), \delta q_2(t), \delta p_2(t), \delta X(t), \delta Y(t)]^{\mathrm{T}},$$
$$n(t) = \left[0, \xi_1(t), 0, \xi_2(t), \sqrt{2\kappa}X^{\mathrm{in}}(t), \sqrt{2\kappa}Y^{\mathrm{in}}(t)\right]$$

represent the vector of input noises, with Hermitian input noise operators $X^{\mathrm{in}} = (c_{\mathrm{in}} + c_{\mathrm{in}}^\dagger)/\sqrt{2}$ and $Y^{\mathrm{in}} = \mathrm{i}(c_{\mathrm{in}}^\dagger - c_{\mathrm{in}})/\sqrt{2}$. The drift matrix A is given by

$$A = \begin{pmatrix} 0 & \omega_1 & 0 & 0 & 0 & 0 \\ -\omega_1 & -\gamma_1 & -\lambda & 0 & G_{\mathrm{m}} & 0 \\ 0 & 0 & 0 & \omega_2 & 0 & 0 \\ -\lambda & 0 & -\omega_2 & -\gamma_2 & 0 & 0 \\ 0 & 0 & 0 & 0 & -\kappa & \Delta \\ G_{\mathrm{m}} & 0 & 0 & 0 & -\Delta_2 & -\kappa \end{pmatrix}, \tag{12}$$

where

$\Delta_2 = \Delta + 2\chi|c_{\mathrm{s}}|^2$,

$G_{\mathrm{m}} = \sqrt{2}gc_{\mathrm{s}} = 2\omega_{\mathrm{c}}/L\sqrt{\kappa P/(m\omega_1\omega_{\mathrm{p}}(\kappa^2+\Delta^2))}$.[58]

Owing to the linearized dynamics and the Gaussian nature of the quantum noises $\xi_{1(2)}$ and c_{in}, the steady state of the quantum fluctuations of the system is a zero-mean bipartite Gaussian state. As a consequence, it is fully characterized by the 6×6 covariance matrix (CM) V with matrix elements,

$$V_{ij} = \left\langle u_i(t)u_j(t') + u_j(t')u_i(t)\right\rangle/2 \quad (i,j = 1,2,\ldots,6). \tag{13}$$

When the system is in the stable limit ($t \to \infty$), we can obtain

$$V_{ij} = \sum_{k,l}\int_0^\infty \mathrm{d}t \int_0^\infty \mathrm{d}t' M_{ik}(t)M_{jl}(t')\phi_{kl}(t-t'), \tag{14}$$

where

$$\phi_{kl}(t-t') = \left(\left\langle n_k(t)n_l(t') + n_l(t')n_k(t)\right\rangle\right)/2$$

is the steady-state noise CM, and $M = \exp(At)$. We can achieve the steady-state CM V by solving the Lyapunov equation[58]

$$AV + VA^{\mathrm{T}} = -D, \tag{15}$$

where $D = \mathrm{diag}[0, \gamma_1(2\bar{n}_1+1), 0, \gamma_2(2\bar{n}_2+1), \kappa, \kappa]$ is the diagonal matrix, which is defined via

$$\left\langle n_i(t)n_j(t') + n_j(t')n_i(t)\right\rangle/2 = D_{ij}\delta(t-t'). \tag{16}$$

Equation (15) is a liner equation for V and can be straightforwardly solved, whereas the explicit expression is too cumbersome and will not be reported here.

To investigate bipartite entanglement of the system, we can trace over the remaining degrees of freedom. Here we adopt the logarithmic negativity E_{N} as a convenient measure of entanglement,[59,60] which is defined as

$$E_{\mathrm{N}} = \max[0, -\ln 2\tilde{\nu}_-], \tag{17}$$

where $\tilde{\nu}_- = \min \mathrm{eig}\left|\mathrm{i}\Omega_2\tilde{V}_4\right|$ is the minimum symplectic eigenvalue of the CM $\tilde{V}_4 = P_{1|2}V_4P_{1|2}$, $\Omega_2 = \oplus_{j=1}^2 \mathrm{i}\sigma_y$ is the symplectic matrix, σ_y is the y-Pauli matrix, and V_4 is the 4×4 CM of two subsystems, which is obtained by disregarding the last two rows and columns in V, and $P_{1|2} = \mathrm{diag}(1,-1,1,1)$ is the matrix that performs partial transposition on CMs.[61]

The stationary entanglement of the system in the steady state is guaranteed when all eigenvalues of the drift matrix A possess negative real parts, which can be derived using Routh–Hurwitz criteria.[62] For numerically illustrating the effect of Kerr medium in a hybrid cavity optomechanical system, a set of experimentally accessible parameters have been taken into account here: $m = 5$ ng, $L = 1$ mm, and $\kappa = 88.1$ MHz.[63,64] For simplicity, we have taken equal parameters of the two NMOs, i.e., $\omega_1 = \omega_2 = \omega_{\mathrm{m}} = 2\pi\times 100$ MHz, $\gamma_1 = \gamma_2 = \gamma_{\mathrm{m}} = 2\pi\times 100$ Hz, and the cavity-field wavelength λ_0 is 810 nm.

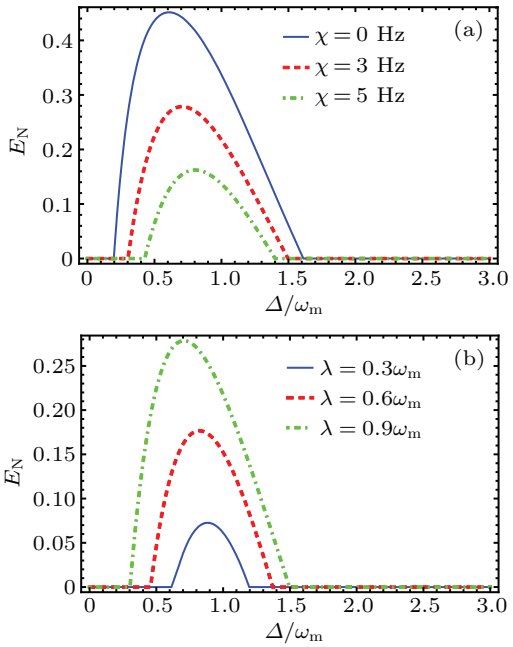


Fig. 2. Logarithmic negativity E_{N} with respect to the normalized detuning $\Delta/\omega_{\mathrm{m}}$ at temperature $T = 4$ mK and driving power $P = 50$ mW. Here we use $\lambda = 0.9\omega_{\mathrm{m}}$ in (a) and $\chi = 3$ Hz in (b). See text for details of the other parameters.

Generally speaking, E_{N} is repressed by the large Kerr parameter χ. The results on the behavior of E_{N} with varying χ are shown in Fig. 2(a), it clearly demonstrates that E_{N} is repressed with increasing χ. In the case of $\chi = 0$, the significant entanglement remains near $\Delta/\omega_{\mathrm{m}} = 0.6$ and for $\chi = 5$ Hz it is shifted towards larger detuning value around $\Delta/\omega_{\mathrm{m}} = 0.8$. More close to the point, with increasing χ, the range of entanglement between two NMOs can be narrowed, i.e., from $\Delta/\omega_{\mathrm{m}} \in [0.2, 1.6]$ (solid line) to $\Delta/\omega_{\mathrm{m}} \in [0.45, 1.4]$

(dot-dashed line). This phenomenon indicates that the photon blockade greatly lowers the number of the cavity photon, which is induced by the Kerr interaction χ, thus E_N can be spoilt when the effective coupling between the two NMOs is weakened, as is shown in Fig. 3, where N is the mean intracavity photon number and is defined as $N = |c_s|^2$.[65] In Fig. 3(a), we can see that negative values of cavity-pump detuning are necessary to observe the optical bistable behavior with the increasing χ. Therefore, we choose $\Delta_c = -3\omega_m$ in Fig. 3(b), and we can observe that N decreases with large χ. In contrast, Fig. 2(b) reflects that E_N is enhanced via increasing the Coulomb coupling parameter λ. The optimal entanglement is shifted from $\Delta/\omega_m = 0.9$ (solid line) to lower detuning value around $\Delta/\omega_m = 0.7$ (dot-dashed line). The effective coupling between the two NMOs is enhanced with increasing the Coulomb coupling strength λ. Simultaneously, the existence region of E_N between the two NMOs can be enlarged, i.e., from $\Delta/\omega_m \in [0.6, 1.2]$ (solid line) to $\Delta/\omega_m \in [0.3, 1.5]$ (dot-dashed line). The wider the effective detuning range is, the easier it is to achieve in experiments. These two figures imply that Kerr interaction χ and Coulomb coupling strength λ are the two main factors affecting the entanglement between the two NMOs. E_N will disappear with large Kerr interaction $\chi = 10$ Hz or small Coulomb coupling strength $\lambda = 0$ (not shown here), respectively.

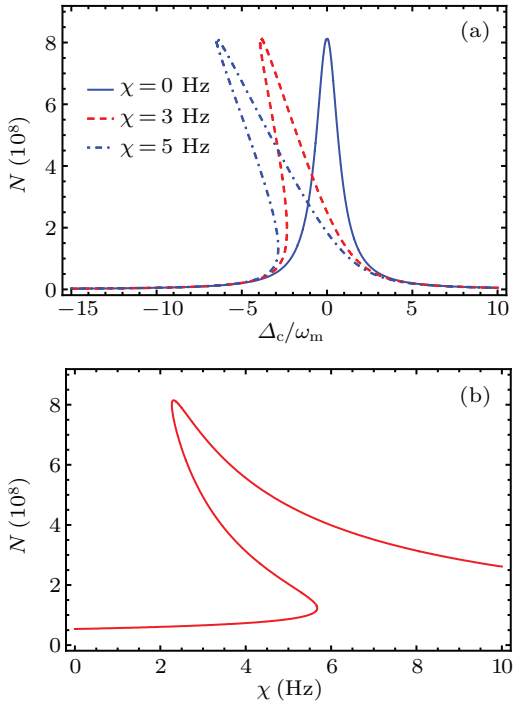


Fig. 3. (a) Mean intracavity photon number as a function of Δ_c with different χ. (b) Mean intracavity photon number as a function of χ with $\Delta_c = -3\omega_m$.

For further investigation about the effect of Kerr interaction χ and Coulomb coupling strength λ on E_N, we plot in Fig. 4(a) E_N versus λ/ω_m and in Fig. 4(b) E_N versus χ respectively. In Fig. 4(a), it clearly displays that the two NMOs are unentangled below a critical Coulomb coupling strength λ_c and E_N monotonically increases with λ in the range $\lambda \in [\lambda_c, \omega_m]$. Critical values $\lambda_{c1} = 0.05\omega_m$ for $\chi = 0$ (solid line), $\lambda_{c2} = 0.13\omega_m$ for $\chi = 3$ Hz (dashed line), and $\lambda_{c3} = 0.29\omega_m$ for $\chi = 5$ Hz (dot-dashed line) are observed. It is obvious from Fig. 4(b) that the two NMOs are disentangled above a critical Kerr interaction χ_c and E_N monotonically decreases with χ in the range $\chi \in [0, \chi_c]$. We find critical Kerr interactions $\chi_{c1} = 5$ Hz for $\lambda = 0.3\omega_m$ (solid line), $\chi_{c2} = 7.2$ Hz for $\lambda = 0.6\omega_m$ (dashed line), and $\chi_{c3} = 9$ Hz for $\lambda = 0.9\omega_m$ (dot-dashed line). E_N decreases with increasing the Kerr interaction due to the photon blockade mechanism. It is worth mentioning that the critical value of Coulomb coupling strength λ_c increases with Kerr interaction χ. Therefore, we infer that when χ increases, λ_c should also increase. Only in this limit can the entanglement between the two NMOs be guaranteed.

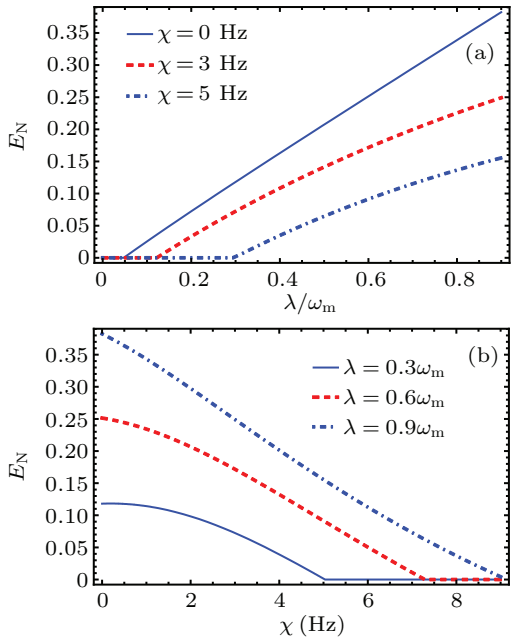


Fig. 4. The logarithmic negativity versus (a) λ/ω_m, and (b) Kerr parameter χ. The parameters are the same as in Fig. 2 but for $\Delta = 0.9\omega_m$.

The dependence of E_N on driving power P, Kerr interaction χ and coupling strength λ are presented in Figs. 5(a) and 5(b), respectively. Apparently, E_N has two distinct behaviors with different driving powers P. In the range $P \in [2\ \text{mW}, 15\ \text{mW}]$, E_N increases very quickly with respect to P. If we continue to increase the driving power P, E_N will decrease gradually. In particular, in Fig. 5(a), E_N increases with Kerr interaction being $\chi = 0$. It is crucial to analyze the robustness of E_N as a function of the environmental temperature T. As shown in Figs. 6(a) and 6(b), we can see the expected decay of E_N for increasing temperature T. In Fig. 6(a), in the absence of Kerr medium, E_N is very robust as a function of T. With the increase of χ, the value and the critical value of temperature T_c decrease (T_c is defined as $T > T_c$, $E_N = 0$). This explains

that the robustness of E_N is inversely correlated with Kerr interaction χ. We can likewise explain the phenomenon in terms of photon blockade. In contrast, it is found from Fig. 6(b) that the value and the critical value of temperature T_c increase with increasing λ. Therefore, the robustness of E_N is enlarged with increasing λ.

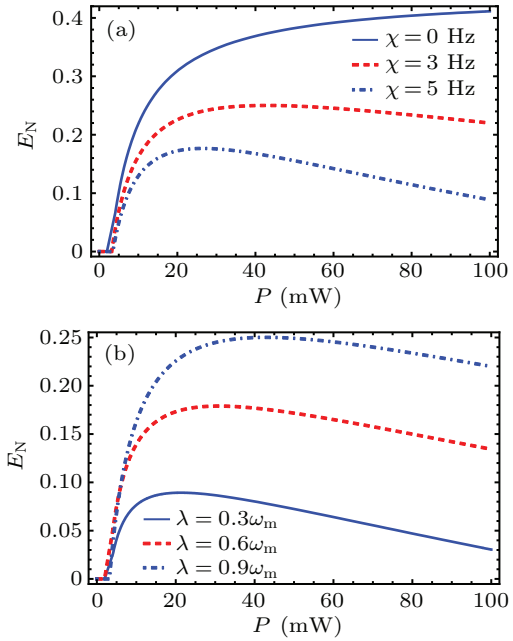


Fig. 5. The logarithmic negativity E_N with respect to the driving power P (mW) at temperature $T = 4$ mK, and normalized detuning $\Delta = 0.9\omega_m$. Here we set $\lambda = 0.9\omega_m$ in (a) and $\chi = 3$ Hz in (b).

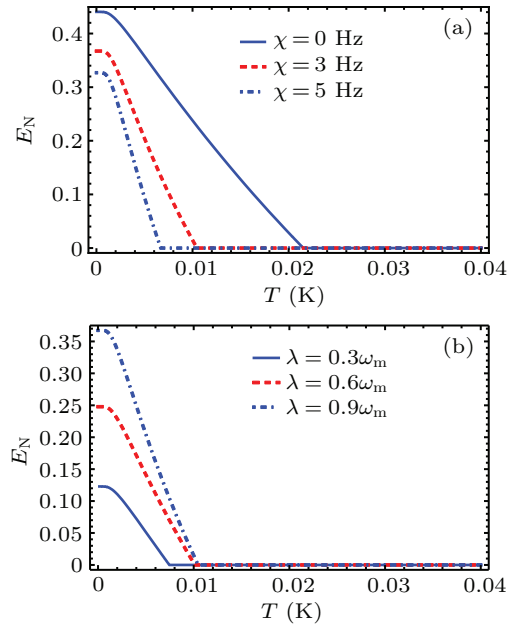


Fig. 6. E_N as a function of the environment temperature T (in units of K). The parameters are the same as in Fig. 5 but for $P = 50$ mW.

In general, lower cavity decay rate κ is needed in an optomechanical system to improve the intracavity photon number. With large cavity decay κ, E_N disappears completely, which can be derived from the steady state solution $c_s = \varepsilon_p/(\kappa + i\Delta)$. The biggest entanglement is obtained near $\kappa/\omega_m = 0.2$ in Fig. 7(a), and the cavity decay κ corresponding to maximal entanglement increases with λ in Fig. 7(b). The range of entanglement can be narrowed, i.e., from $\kappa/\omega_m \in [0.03,\ 0.9]$ (solid line) to $\kappa/\omega_m \in [0.03,\ 0.8]$ (dot-dashed line) with increasing χ. In contrast, the range of entanglement can be enlarged greatly with λ.

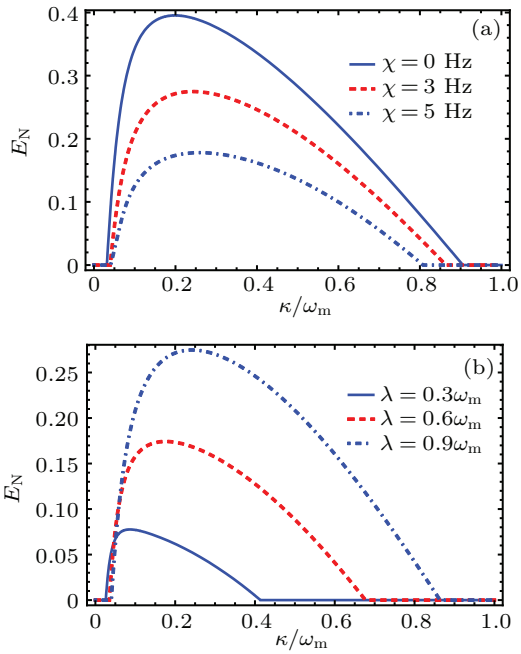


Fig. 7. E_N versus cavity decay rate κ/ω_m. Other parameters are the same as in Fig. 5 but for $P = 50$ mW.

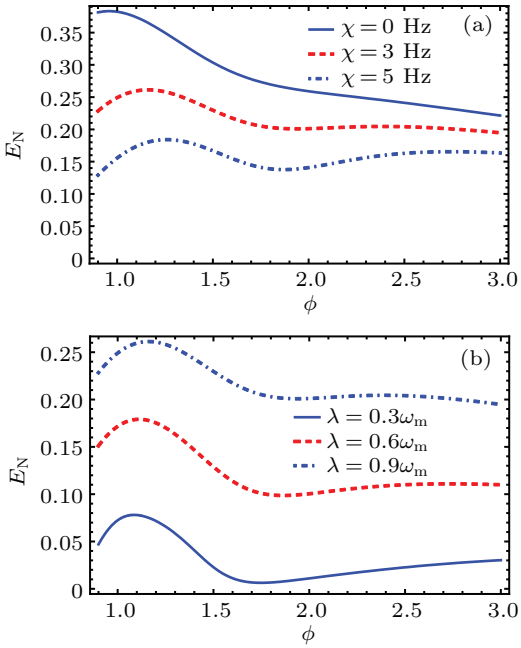


Fig. 8. E_N with respect to frequency ratio ϕ when the two charged NMOs have different frequencies ($\omega_2 = \phi\omega_1$). The rest of the parameters are $P = 50$ mW and $T = 4$ mK.

In fact, identical frequencies of two NMOs are hard to be guaranteed. Therefore, one important task is to analyze E_N in the general case of frequency ratio $\phi \neq 1$. The maximal entanglement occurs only in the small range around $\phi = 1$, as shown

in Figs. 8(a) and 8(b), which means that the difference in frequency values between two NMOs should not be significant. Figure 8(a) partly reflects that without the Kerr interaction χ, the maximal entanglement between the two charged NMOs is obtained when $\phi = 1$. With increasing χ, the value of maximal entanglement decreases, and the maximal entanglement only occurs for higher value of ϕ ($\omega_2 > \omega_1$). In Fig. 8(b), the maximal entanglement is obtained when $\phi = 1.1$, and the entanglement increases with λ. However, the optimal entanglement corresponds to the identical value of ϕ while varying λ. On the contrary, the Kerr interaction χ can change the value of ϕ corresponding to optimal entanglement.

We plot E_N in Fig. 9 for the NMO-NMO entanglement in the case of different decay rates of two NMOs. The entanglement is anti-correlation with Γ, and therefore the decay rate of NMO_1 should be larger than the decay rate of NMO_2 to attain optimal entanglement. In this case, the maximal entanglement appears at $\Gamma = 0$. The above discussion implies that the NMO-NMO entanglement can be enhanced by the decay rate of NMO_1 and Coulomb coupling strength λ. The entanglement will decrease if the Kerr interaction χ increases in terms of photon blockade mechanism.

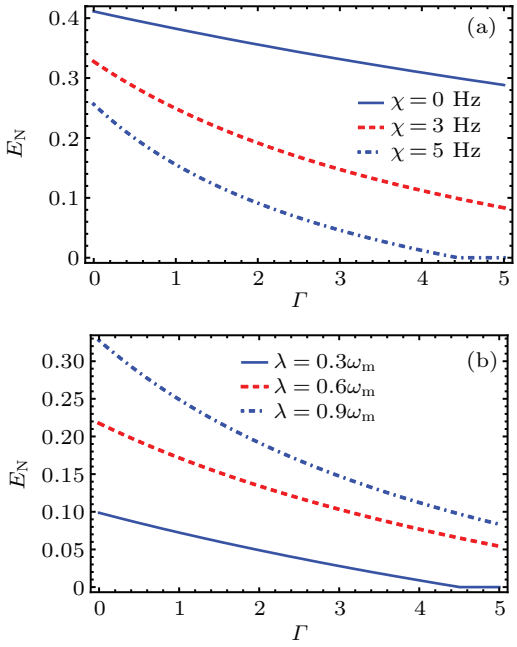


Fig. 9. E_N with respect to decay rate ratio Γ when the two charged NMOs have different decay rates ($\gamma_2 = \Gamma\gamma_1$). The rest of the parameters are $P = 50$ mW, $\phi = 1$ and $T = 4$ mK.

Lastly, we present the entanglement between cavity and NMO_1. Here V_4 should be changed, which is obtained by disregarding the third and fourth rows and columns in V. In this three-mode hybrid system, the entanglement between two NMOs is stronger than that between the cavity and NMO_1. Simultaneously, the entanglement between the cavity and NMO_2 is too weak (10^{-7} in order of magnitude) and will not be demonstrated here. Figure 10 clearly displays that the degree of entanglement between the cavity and NMO_1 is very small. Here, the effects of χ and λ are similar to the cases in Fig. 2. It is worth noting that g is the coupling parameter between NMO_1 and the cavity field. Heightening the value of ϕ, the value of g will increase, and then the entanglement between the cavity and NMO_1 will be enhanced.

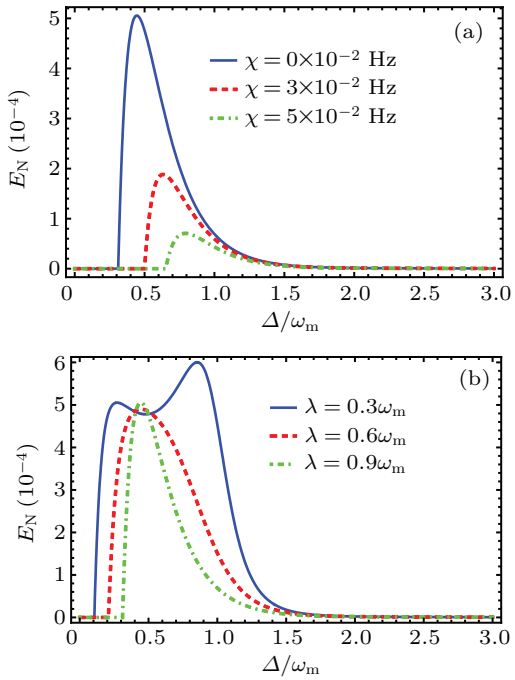


Fig. 10. E_N between the Fabry–Pérot cavity and NMO_1 with respect to the normalized detuning Δ/ω_m. We adopt $\chi = 0$ in (b). Other parameters are consistent with those in Fig. 2.

4. Conclusion

In summary, we have presented the NMO-NMO entanglement in an optomechanical system with a Kerr medium and two charged NMOs, where one oscillator is coupling to another oscillator via Coulomb interaction. Using possible strategies to measure the entanglement, we find that the generated entanglement can be controlled by adjusting the Kerr interaction, Coulomb coupling strength and the frequency ratio of two NMOs. The maximal entanglement can be obtained when the decay rate of NMO_1 is larger than the decay rate of NMO_2 ($\gamma_2 < \gamma_1$). The NMO-NMO entanglement is spoilt by Kerr interaction due to the photon blockade mechanism. In contrast to the case with Kerr interaction, the Coulomb coupling strength can enhance the NMO-NMO entanglement due to stronger effective coupling between two NMOs. Moreover, Kerr interaction has an important influence on changing the values of cavity decay rate and frequency ratio of two NMOs corresponding to maximal entanglement. Our results indicate that this hybrid optomechanical system could provide a promising platform for research of macroscopic quantum phenomena.

References

[1] Heilmann R, Gräfe M, Nolte S and Szameit A 2015 *Sci. Bull.* **60** 96
[2] Wu Y L, Li S J, Ge W, Xu Z X, Tian L and Wang H 2015 *Sci. Bull.* **61** 302
[3] Xu X X 2015 *Phys. Rev. A* **92** 012318
[4] Yu Y B, Ji F M, Shi Z T, Wang H J, Zhao J W and Wang Y J 2017 *Laser Phys. Lett.* **14** 035202
[5] Wang C, Shen W W, Mi S C, Zhang Y and Wang T J 2015 *Sci. Bull.* **60** 2016
[6] Zhang X, Chen Y H, Wu Q C, Shi Z C, Song J and Xia Y 2017 *Laser Phys.* **27** 015202
[7] Pirandola S, Eisert J, Weedbrook C, Furusawa A and Braunstein S L 2015 *Nat. Photon.* **9** 641
[8] Horodecki R, Horodecki P, Horodecki M and Horodecki K 2009 *Rev. Mod. Phys.* **81** 865
[9] Leggett A J 1980 *Prog. Theor. Phys.* **69** 80
[10] Zurek W H 1991 *Phys. Today* **44** 36
[11] Du S J, Peng Y G, Feng H R, Han F, Yang L W and Zheng Y J 2020 *Chin. Phys. B* **29** 074202
[12] Kimble H J 2008 *Nature* **453** 1023
[13] Einstein A, Podolsky B and Rosen N 1935 *Phys. Rev.* **47** 777
[14] Liu J H, Zhang Y B, Yu Y F and Zhang Z M 2019 *Front. Phys.* **14** 12601
[15] Tan J and Fang M F 2006 *Chin. Phys.* **15** 2514
[16] Li H M, Xu X X, Yuan H C and Meng X G 2019 *Laser Phys. Lett.* **16** 105202
[17] Zhang G F, Yin W, Liang J Q and Yan Q W 2004 *Chin. Phys.* **13** 988
[18] Yuan H C, Wang Z, Chen Q M and Dou X M 2015 *Mod. Phys. Lett. A* **30** 1550109
[19] Liao Q H and He G Q 2020 *Quantum Inf. Process* **19** 91
[20] Ke Z J, Wang Y T, Yu S, Liu W, Meng Y, Li Z P, Wang H, Li Q, Xu J S, Xiao Y, Tang J S, Li C F and Guo G C 2020 *Chin. Phys. B* **29** 080301
[21] Li X M, Chen Y X, Xia Y J, Zhang Q and Man Z X 2020 *Chin. Phys. B* **29** 060302
[22] Marshall W, Simon C, Penrose R and Bouwmeester D 2003 *Phys. Rev. Lett.* **91** 159903
[23] Li J, Zhu S Y and Agarwal G S 2018 *Phys. Rev. Lett.* **121** 203601
[24] Zheng L L, Yin T S, Bin Q, Lü X Y and Wu Y 2019 *Phys. Rev. A* **99** 013804
[25] Schwab K C and Roukes M L 2005 *Phys. Today* **58** 36
[26] Kippenberg T J and Vahala K J 2008 *Science* **321** 1172
[27] Marquardt F and Girvin S M 2009 *Physics* **2** 40
[28] Verlot P, Tavernarakis A, Briant T, Cohadon P F and Heidmann A 2010 *Phys. Rev. Lett.* **104** 133602
[29] Mahajan S, Kumar T, Bhattacherjee A B and ManMohan 2013 *Phys. Rev. A* **87** 013621
[30] Xiong H, Gan J H and Wu Y 2017 *Phys. Rev. Lett.* **119** 153901
[31] Teufel J D, Donner T, Castellanos-Beltran M A, Harlow J W and Lehnert K W 2009 *Nat. Nanotechnol.* **4** 820
[32] Wilson D J, Regal C A, Papp S B and Kimble H J 2009 *Phys. Rev. Lett.* **103** 207204
[33] Liao Q H, Xiao X, Nie W J and Zhou N R 2020 *Opt. Express* **28** 4
[34] Thompson J D, Zwickl B M, Jayich A M, Marquardt F, Girvin S M and Harris J G E 2008 *Nature* **452** 72
[35] Sohail A, Rana M, Ikram S, Munir T, Hussain T, Ahmed R and Yu C S 2020 *Quantum Inf. Process* **19** 372
[36] Craddock A N, Hannegan J, Ornelas-Huerta D P, Siverns J D, Hachtel A J, Goldschmidt E A, Porto J V, Quraishi Q and Rolston S L 2019 *Phys. Rev. Lett.* **123** 213601
[37] Zou F, Lai D G and Liao J Q 2020 *Opt. Express* **28** 16175
[38] Liew T C H and Savona V 2010 *Phys. Rev. Lett.* **104** 183601
[39] Lü X Y, Zhang W M, Sahel Ashhab, Wu Y and Franco Nori 2013 *Sci. Rep.* **3** 2943
[40] Mikkelsen M, Fogarty T, Twamley J and Busch Th 2017 *Phys. Rev. A* **96** 043832
[41] Wang K, Wu Q, Yu Y F and Zhang Z M 2019 *Phys. Rev. A* **100** 053832
[42] Kumar T, Bhattacheriee A B and ManMohan 2010 *Phys. Rev. A* **81** 013835
[43] Bin Q, Lü X Y, Bin S W and Wu Y 2018 *Phys. Rev. A* **98** 043858
[44] Chen W J, Song D, Li Y, Wang X, Qin X L and Liu C Y 2019 *Acta Phys. Sin.* **68** 094206 (in Chinese)
[45] Zhang D, Zhang X P and Zheng Q 2013 *Chin. Phys. B* **22** 064206
[46] Zhou L, Han Y, Jing J T and Zhang W P 2011 *Phys. Rev. A* **83** 052117
[47] Zhang D and Zheng Q 2013 *Chin. Phys. Lett.* **30** 024213
[48] Löw U, Emery V J and Fabricius K 1994 *Phys. Rev. Lett.* **72** 1918
[49] Bohm D and Pines D 1953 *Phys. Rev.* **92** 609
[50] Ma P C, Zhang J Q, Xiao Y, Feng M and Zhang Z M 2014 *Phys. Rev. A* **90** 043825
[51] Wu Q, Xiao Y and Zhang Z M 2016 *Chin. Phys. B* **25** 014203
[52] Imamoglu A, Schmidt H, Woods G and Deutsch M 1997 *Phys. Rev. Lett.* **79** 1467
[53] Mu Q X and Lin P Y 2020 *Chin. Phys. B* **29** 060304
[54] Mancini S and Tombesi P 1994 *Phys. Rev. A* **49** 4055
[55] Zhang L W, Li X L and Yang L 2019 *Acta Phys. Sin.* **68** 170701
[56] Genes C, Vitali D, Tombesi P, Gigan S and Aspelmeyer M 2008 *Phys. Rev. A* **77** 033804
[57] Xiao Y M, Liu J H, Wu Q, Yu Y F and Zhang Z M 2020 *Chin. Phys. B* **29** 074204
[58] Vitali D, Gigan S, Ferreira A, Böhm H R, Tombesi P, Guerreiro A, Vedral V, Zeilinger A and Aspelmeyer M 2007 *Phys. Rev. Lett.* **98** 030405
[59] Plenio M B 2005 *Phys. Rev. Lett.* **95** 090503
[60] Vidal G and Werner R F 2002 *Phys. Rev. A* **65** 032314
[61] Simon R 2000 *Phys. Rev. Lett.* **84** 2726
[62] DeJesus E X and Kaufman C 1987 *Phys. Rev. A* **35** 5288
[63] Schliesser A, Riviere R, Anetsberger G, Arcizet O and Kippenberg T J 2008 *Nat. Phys.* **4** 415
[64] Gigan S, Böhm H R, Paternostro M, Blaser F, Langer G, Hertzberg J B, Schwab K C, Bäuerle D, Aspelmeyer M and Zeilinger A 2006 *Nature* **444** 67
[65] Wang Z, Jiang C, He Y, Wang C Y and Li H M 2020 *Nature* **37** 579